Optimization of the shear stress induced by ultrasonically-stimulated oscillating MBs: A theoretical investigation

Amin Jafari Sojahrood, Raffi Karshafian, and Michael C. Kolios

Citation: AIP Conf. Proc. **1481**, 351 (2012); doi: 10.1063/1.4757360
View online: http://dx.doi.org/10.1063/1.4757360
View Table of Contents: http://proceedings.aip.org/dbt/dbt.jsp?KEY=APCPCS&Volume=1481&Issue=1
Published by the American Institute of Physics.

Optimization of the Shear Stress Induced by Ultrasonically-Stimulated Oscillating MBs: A Theoretical Investigation

Amin Jafari Sojahrood, Raffi Karshafian, and Michael C. Kolios

Department of Physics, Ryerson University, Toronto, Ontario Canada

Abstract. Shear stress induced by ultrasonically-stimulated MBs has been associated with sonoporation and sonothrombolysis. In this study, the dynamics of oscillating MBs is investigated numerically using the Hoff model for varying parameters (MB radius (Ro), pulse frequency and acoustic pressure) and the average shear stress was calculated using the Rooney model. The MB oscillations were maintained below a normalized radial oscillation of two to avoid inertial cavitation. The simulations demonstrated that the shear stress induced by MBs increased significantly at exposure frequencies of non-integer multiples of the resonance frequency (fr), only above a pressure threshold. The pressure threshold, located at the saddle node bifurcation point where the MB oscillation increases suddenly, depended on MB size, pulse frequency and shell properties. The shear stress induced by a 4 um oscillating MB increased by 10-fold when exposed to 8.85 MHz (2.93fr) compared to the maximum shear stress at the MB resonance frequency (3.02 MHz). This increase is concomitant with the saddle node bifurcation in normalized radial oscillations from 1.12 to 1.69 at 1.53 MPa. In conclusion, ultrasound exposure frequency and acoustic pressure can be tailored to maximize and control the shear stress induced by MBs undergoing stable oscillation for optimizing ultrasound therapeutic bioeffects.

Keywords: MBs, Shear Stress, Ultrasound Bioeffects

INTRODUCTION

The application of ultrasound and microbubbles (MBs) can temporarily increase the permeability of cell membranes, a phenomenon known as sonoporation. This allows the passage of macromolecules into the intracellular space of cells which otherwise would be excluded. The underlying biological mechanism has been postulated to be disruption and pore formation on the plasma membrane [1], which reseal within minutes following the end of the ultrasound exposure. The presence of MBs appears to be important in enhancing cell permeability. Although sonoporation can be induced at high pressures [1], the mechanism has been attributed to cavitation[2].

MBs placed in an ultrasound field will undergo stable oscillation and inertial cavitation depending on the ultrasound exposure conditions and MB characteristics. As a result of micro streaming due to the bubble oscillations, shear stress will be exerted on cell membranes of nearby cells, which leads to the increased permeability of the cells [3,4]. The magnitude of this shear stress is closely related to the frequency and amplitude of the radial oscillations of the bubble.

11th International Symposium on Therapeutic Ultrasound
AIP Conf. Proc. 1481, 351-356 (2012); doi: 10.1063/1.4757360

Due to the complex and nonlinear bubble behavior which depends on parameters related to the ultrasonic exposure (frequency and pressure) and the MB properties (size and shell parameters), understanding the impact of the nonlinear oscillations on the amount of generated shear stress is important. Such an understanding will help designing the treatment parameters in a more efficient manner (e g. by enhancing the shear stress) and provide the theoretical basis to better understand the mechanism of therapeutic procedures like sonoporation, blood brain barrier opening or thrombolysis.

The hypothesis guiding this study is that the shear-stress generated by oscillating MBs can be enhanced through ultrasound exposure frequency and pressure, and MB size. The specific objectives of this study were (1) to model the radial oscillation of MBs under varying ultrasound frequency and acoustic pressure, (2) to investigate the response of MBs varying in size, and (3) to determine the shear-stress generated by oscillating MBs.

METHODS

The radial oscillations were calculated using the Hoff model [5]:

$$\rho_L R\ddot{R} + \frac{3}{2}\rho_L \dot{R}^2 = P_0\left(\frac{R_0}{R}\right)^{3\gamma} - 4\eta_L\frac{\dot{R}}{R} - 12\eta_s\frac{d_s R_0^2}{R^3}\frac{\dot{R}}{R} - 12G_s\frac{d_s R_0^2}{R^3}\left(1-\frac{R_0}{R}\right) - P_0 - P_{\mathrm{drive}}(t). \tag{1}$$

where R_0 is the bubble initial radius, ρ_L liquid density, η_s and η_L shell and liquid viscosities, P_0 pressure inside the bubble, d_s shell thickness and G_S shell shear modulus and γ is the polytropic gas exponent. $P_{drive}(t)= P_a sin(2\pi\, \upsilon\, t)$ where P_a is the acoustic pressure and υ is frequency.

A variety of MB parameters (R_0 = 0.5-5μm G_S= 8MPa-200MPa and d_s=1nm-20nm) were considered. For each case, the multiple frequencies (f=0.5-3 times the bubble resonance frequency (fr), were employed and the dynamics of the bubble was studied for a wide range of pressures at each frequency. For a given bubble and frequency, the simulation stopped when the maximum bubble oscillations increased above twice the initial bubble radius. The analysis of the dynamics were done through plotting the bifurcation diagrams of the normalized bubble oscillations (NBOA=Rmax/R0) versus applied pressure. The procedure for generating the bifurcation diagrams is presented in other publications [6, 7]. The bifurcation diagrams were calculated for the last 40 cycles of an 80 cycle sonication.

Afterwards, the shear stress resulting on a nearby cell was calculated using the following equation from Rooney [8]:

$$S = \eta G = \frac{2\pi^{\frac{3}{2}}{\epsilon_0}^2(\rho\nu^3\eta)^{\frac{1}{2}}}{R_0} \tag{2}$$

The maximum shear stress of the bubble oscillations was also calculated for the last 40 stable cycles. Afterwards, the corresponding time averaged shear stress was calculated for the whole 80 cycles and the results were compared.

RESULTS AND DISCUSSION

The normalized bifurcation diagram of 2 μm radius microbubble exposed to 2.24 MHz, 3.02 MHz (resonance frequency), 5.58 MHz and 8.85 MHz for pressures up to destruction threshold amplitude is shown in Figure 1. The microbubble simulation parameters were Gs=50 MPa and epsilon=3 nm with mush=0.70. The dynamics of the microbubble demonstrated a pressure dependent behaviour at frequencies that were non-integer multiples of the resonance frequency. At 2.25 MHz frequency (> resonance frequency) (black colour), the microbubble radial oscillation increased significantly as the pressure exceeded 100 kPa amplitude. The disruption threshold

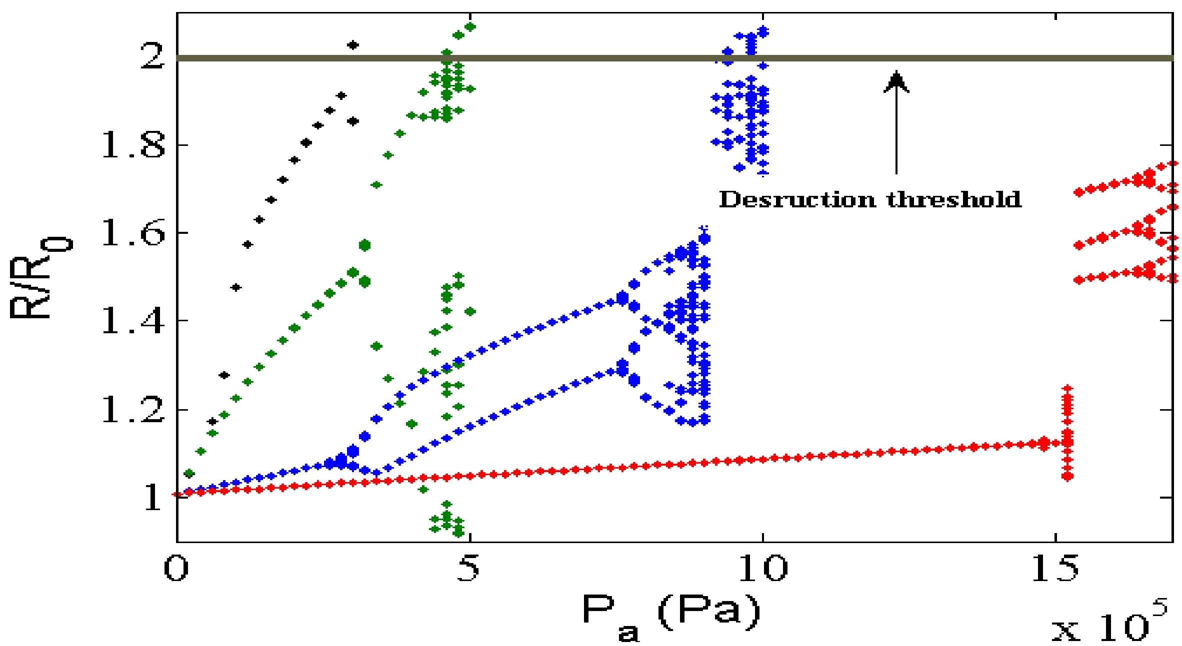

FIGURE 1. Maximum normalized oscillations of a bubble versus driving pressure when the driving frequency is: a) 2.25MHz (black), b) 3.02 MHz (green), c) 5.85 MHz (blue) and d) 8.85 MHz (red).

pressure at 2.25 MHz was 300 kPa. At the resonance frequency (3.02 MHz) (green colour), the microbubble oscillation increased linearly with acoustic pressure up to 310 kPa where the microbubble exhibited period doubling (the occurrence of two maxima in the microbubble oscillation). The disruption threshold at resonance frequency was 450 kPa. At frequencies (5.8 MHz) higher than the resonance frequency (3.02 MHz), the microbubble oscillation increased linearly with pressure up to 260 kPa above which microbubble exhibited period doubling. At 8.85 MHz frequency (red colour), the microbubble exhibited low amplitude oscillation up to 1.5

MPa above which micorubble radial oscillation demonstrated large non-linear oscillation of period 3. The normalized radial oscillation increased from 1.13 to 1.69. At 1.7 MPa, which is lower than the disruption threshold at 8.85 MHz, the microbubble oscillation amplitude was 1.8 (normalized radial oscillation), and above which the microbubbles underwent chaotic oscillations.

As a discussion of the results of this part, as seen the oscillations of the MBs are pressure dependent. Especially in case of sonications with frequencies less than integer multiples of the resonance frequency, driving the bubble above a pressure threshold will lead to large NBOA. This shows that for each frequency, the applied acoustic pressure should be optimized properly to be able to significantly increase the

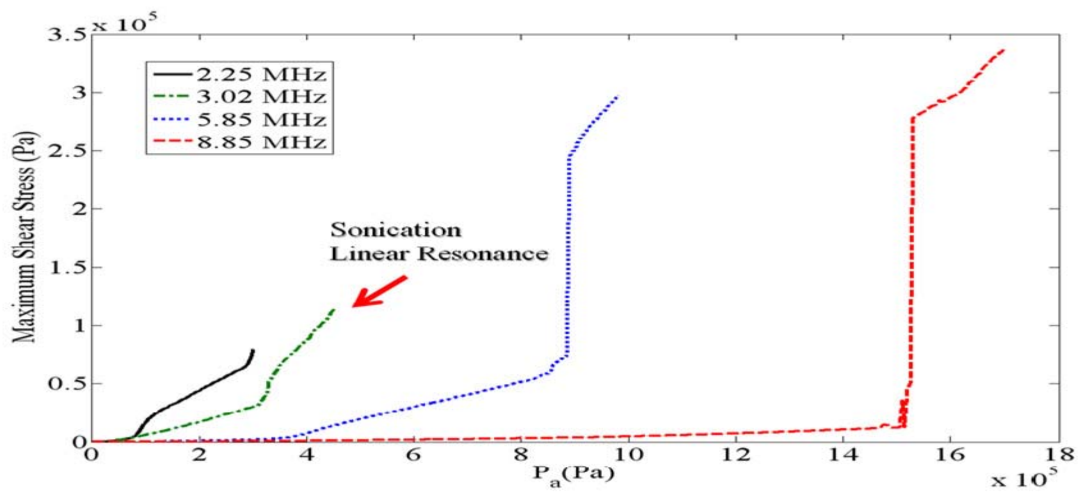

FIGURE 2. Maximum shear stress versus acoustic pressure when the driving frequency is: 2.24 MHz (black), 3.02 MHz (green), 5. 8 MHz (blue) and 8.85 MHz (red).

stable MB oscillation amplitude. On the other hand (comparison between green and black), if there is a limitation in increasing the pressure, through optimizing the suitable frequency the NBOA can be maximized.

Figure 2 shows the maximum shear stress (MSS) generated by MB pulsations in Fig. 1. The MSS follows the same pattern of the radial oscillations. However, there are striking differences between the magnitudes of the shear stress. When the MB is driven with 2.24 MHz which is less than its resonance frequency, the MSS is less than the case of ν=3.02 MHz; only below a pressure threshold. As soon as the pressure is increased above the threshold, the oscillation becomes stronger and the MSS becomes larger than the case of ν=3.02 MHz. However, the bubble finally loses stability and will collapse at 300 kP. The MSS at the point of collapse is 66.25 kPa. At the same acoustic pressure, the MSS is 30 kPa when ν=3.02 MHz. For ν=3.02 MHz, as the acoustic pressure increases the NBOA becomes larger. At the point of collapse (Pa=450 KPa) the MSS is 113.5 kPa which is higher than the case of applying f=2.24 MHz. As seen in Fig. 2, when ν=5.8 MHz, the MSS is much smaller than the case of ν=3.02 MHz, again only below a pressure threshold. At the pressure threshold of ~890 kPa a saddle node bifurcation takes place in radial oscillations and the amplitude of normalized oscillations jumps from to 1.5 to 1.9. This is concomitant with a large increase in the MSS from 74 kPa to 245 kPa. Finally bubble loses stability at 980 kPa and collapses. The maximum achievable shear stress in this case is 297 kPa. The same phenomenon is observed for ν=8.85 MHz (red line in Fig. 2). The MSS is very small below a pressure threshold of 1.52 MPa. As soon as the acoustic pressure increases above this threshold, the maximum shear stress jumps from 12.6 kPa (Pa=1.51MPa) to 280 kPa (Pa=1.53 MPa) which is more than a 10 fold increase. The MSS before chaotic oscillations and bubble destruction reaches to 337 kPa.

In order to have a better measure of the shear stress, the time averaged shear stress (TASS) for the entire period of bubble oscillation should be considered. This is because in some instances, subharmonics appear in the MB pulsations. The occurrence of subharmonics is associated with the creation of secondary and tertiary maxima in the bubble oscillations with amplitudes less than the maximum oscillation amplitude. Thus, the bubble cannot maintain the maximum shear stress in every cycle. Therefore, the total TASS can be a better measure of the effective shear stress on a nearby membrane. The TASS of the whole 80 cycles is plotted in Fig 3. The same trend of pressure dependent behavior exists in cases of sonications with frequencies which are less than the integer multiples of the resonance frequency of the MB. However, although the maximum achievable shear stress is higher for ultrasound exposures at 3.02 MHz compared to 2.24 MHz, the maximum achievable TASSs before bubble destruction are almost equal. The maximum achievable TASS is approximately 29 kPa. For ν =5.8 and 8.85 MHz and after the pressure passes the threshold, the TASS jumps to a higher value. In case of ν =5.8 MHz the TASS jumps from 30.1 kPa to 104.5 kPa when the pressure increases above 890 kPa. When driving the bubble with 8.85 MHz; the shear stress jumps from 26.1 kPa to 115 kPa as soon as the pressure is elevated above 1.53 MPa. The maximum achievable TASSs before bubble destruction are respectively 117 kPa and 131 kPa for ν =5.8 and 8.85 MHz.

In discussion, The MSS and TASS resulted by MB oscillations on a nearby membrane are frequency and pressure dependent. High frequency sonication (at multiples of the bubble resonance frequency) combined with the right pressure may increase the efficacy of the sonoporation because of the higher generated stress. Another advantage of higher MSS in this regime is that, inertial cavitation is avoided as the NBOA can be kept below destruction threshold. Therefore, a very high shear stress can be maintained for a long duration of the treatment. Higher sonoporation efficiency at high frequencies has also been observed experimentally [9]. In certain applications where low shear stress is needed or for long sonication times, the sudden change in microbubble behavior may be undesirable and should be avoided. For low pressure applications where high shear stress is needed the appropriate pressure dependent resonance (frequencies below linear resonance frequency of the bubble) should be employed to maximize the shear stress. The effect of pressure depended resonance has also been reported in [4]. The wrong choice of frequency or pressure can severely impair the treatment efficacy as very high or very low shear stresses can be generated.

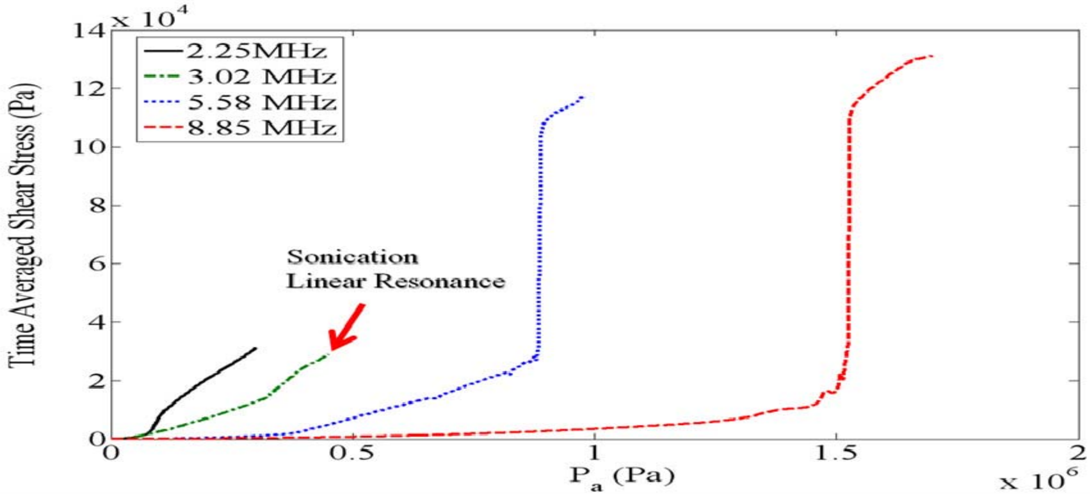

FIGURE 3. Time averaged shear stress versus acoustic pressure when the driving frequency is: 2.24 MHz (black), 3.02 MHz (green), 5. 8 MHz (blue) and 8.85 MHz (red).

CONCLUSION

In conclusion, ultrasound exposure frequency and acoustic pressure can be tailored to maximize and control the shear stress induced by MBs undergoing stable oscillations for optimizing ultrasound therapeutic bioeffects. In this regard, fully classification of the dynamics of the MBs especially at frequencies higher than its resonance will help to better understand the procedure and optimize the sonication parameters

REFERENCES

1. R. Karshafian et al., *Ultrasound Med. Biol*. **35,** 847-860 (2009).
2. L. D. Miller et al., *Somatic Cell and Molecular Genetics*, **27**, 115-134 (2002).
3. J. Wu, *Progress in Biophysics and Molecular Biology* 93 363–373 (2007).
4. J. Wu, *Ultrasound Med. Biol*. **28**, 125–129 (2002).
5. L. Hoff, P. C. Sontum and J. M. Hovem, *J. Acoust. Soc. Am*. **107,** 2272- 2280(2000).
6. G. Simon, P. Cvitanovic, M. T. Levinsen, I. Csabai and A. Horvath, *Nonlinearity* **15,** 2543(2002).
7. S. Behnia, A. J. Sojahrood, W. Soltanpoor and O. Jahanbakhsh, *Ultrasonics Sonochemistry* **16,** 502-511 (2009).
8. J. A. Rooney, *Science* **169**, 869–871 (1970).
9. M. M. Forbes, L. Ryan, L. Steinberg and W. D. O'Brien, Jr., *J. Ultrasound Med*. **30** 61-69 (2011).